Nanoscale

COMMUNICATION

View Article Online
View Journal | View Issue

Cite this: *Nanoscale*, 2019, **11**, 14141

Received 16th March 2019,
Accepted 15th July 2019

DOI: 10.1039/c9nr02297j

rsc.li/nanoscale

Ionizable amino lipid interactions with POPC: implications for lipid nanoparticle function†

M. Ramezanpour, [a] M. L. Schmidt,[b] I. Bodnariuc, [c,d] J. A. Kulkarni, [e,f] S. S. W. Leung, [b] P. R. Cullis, [e] J. L. Thewalt [b,c] and D. P. Tieleman *[a]

Lipid nanoparticles (LNPs) composed of ionizable cationic lipids are currently the leading systems for siRNA delivery in liver disease, with the major limitation of low siRNA release efficacy into the cytoplasm. Ionizable cationic lipids are known to be of critical importance in LNP structure and stability, siRNA entrapment, and endosomal disruption. However, their distribution inside the LNPs and their exact role in cytoplasmic delivery remain unclear. A recent study [Kulkarni *et al.*, On the formation and morphology of lipid nanoparticles containing ionizable cationic lipids and siRNA, *ACS Nano*, 2018, 12(5), 4787–4795] on LNP-siRNA systems containing the ionizable lipid DLin-KC2-DMA (also known as KC2 with an apparent pK_a of *ca.* 6.7) suggested that neutral KC2 segregates from other components and forms an amorphous oil droplet in the core of LNPs. In this paper, we present evidence supporting the model proposed by Kulkarni *et al.* We studied KC2 segregation in the presence of POPC using molecular dynamics simulation, deuterium NMR, SAXS, and cryo-TEM experiments, and found that neutral KC2 has a high tendency to separate from POPC dispersions. KC2 confinement, upon raising the pH during the formulation process, could result in rearrangement of the internal structure of LNPs. As interactions between cationic KC2 and anionic endosomal lipids are thought to be a key factor in cargo release, KC2 confinement inside the LNP may be responsible for the observed low release efficacy.

Introduction

Lipid nanoparticles (LNPs) containing ionizable cationic lipids (ICLs) are among the leading drug delivery system candidates with promising applications for siRNA and mRNA delivery.[1–4] One current limitation of these systems is the low release efficacy of siRNA, which has been estimated to be 1–2%.[5,6] Transfection efficacy can be affected to a considerable extent by LNP size, surface composition, interior lipid distribution, as well as internal structure.[2,7–9] The ICL component of these LNP–siRNA systems, with an apparent pK_a of less than 7.0,[10] plays a critical role in siRNA entrapment, internal arrangement of biomolecules in the LNPs, and endosomal escape of the therapeutics.

DLin-KC2-DMA, also known as KC2, is an optimized ICL with a reported apparent pK_a of 6.7.[10,11] This pK_a ensures an efficient encapsulation of nucleic acid polymers at low pH, a nearly neutral surface charge for the LNPs in the circulation at physiological pH, and a high positive surface charge at endosomal pH. Electrostatic interactions between cationic lipids and naturally occurring anionic lipids in endosomal membranes have been proposed as the underlying mechanism of drug release for LNPs containing (ionizable) cationic lipids.[2,10,12] Thus, the presence of protonated KC2 on the LNP surface is assumed to be required for destabilizing the endosomal membrane and releasing siRNA. However, there are still discrepancies regarding the detailed internal structure and lipid distribution across this class of LNPs.[2,13,14] Previous work, using cryo-TEM, has shown that LNP–siRNA systems containing KC2 form structures with electron dense cores.[7,13–16] This electron-dense core was hypothesized to be the result of inverted micellar structures enclosing siRNA molecules generated through rapid-mixing procedure.[13,15] More recently, it was determined that LNPs containing KC2 generated liposomal structures when the KC2 is protonated at pH 4, while forming electron-dense structures at pH 7.4.[14] This suggests that KC2 might adopt an oil-phase when neutralized.

[a]*Centre for Molecular Simulation, Department of Biological Sciences, University of Calgary, Calgary, AB T2N 1N4, Canada. E-mail: tieleman@ucalgary.ca*
[b]*Department of Physics, Simon Fraser University, Burnaby, BC V5A 1S6, Canada*
[c]*Department of Molecular Biology and Biochemistry, Simon Fraser University, Burnaby, BC V5A 1S6, Canada*
[d]*Department of Chemistry, University of Calgary, Calgary, AB T2N 1N4, Canada*
[e]*Department of Biochemistry and Molecular Biology, University of British Columbia, Vancouver, BC V6 T 1Z3, Canada*
[f]*Department of Medical Genetics, University of British Columbia, Vancouver, BC V6 T 1Z3, Canada*

†Electronic supplementary information (ESI) available: Table summarizing all systems simulated, details on methods and analysis, details of the parameterization of KC2 and KC2H, and additional discussion. See DOI: 10.1039/c9nr02297j

Understanding the structural properties of LNPs is difficult due to the inherently complex nature of LNP manufacturing. To what extent are the fundamental interactions between ionizable cationic lipids such as KC2 and phospholipids responsible for the sequestration of neutral KC2 away from other typical LNP constituents such as phosphatidylcholine? In this study we used molecular dynamics (MD) simulation, solid state deuterium nuclear magnetic resonance (^{2}H NMR) and small angle X-ray scattering (SAXS) experiments to investigate the interactions between KC2 and POPC as a function of pH, temperature and mixing ratio. Additionally, we performed cryo-TEM experiments on LNPs composed of POPC, KC2 and cholesterol to investigate KC2 localization in LNPs and simulations of the same mixture.

Methods

The deuterium order parameter (S_{CD}) profile for the POPC palmitoyl chain in POPC/KC2 and POPC/KC2H bilayers was measured from ^{2}H NMR and used to validate force field parameters for simulations of KC2. Both KC2 and its protonated state (KC2H) were parametrized using the CHARMM36 force field (C36 FF).[17] Bilayers composed of POPC and KC2 or KC2H were simulated, and the S_{CD} profiles for the POPC palmitoyl acyl chain obtained from simulations were compared with the corresponding profiles extracted from ^{2}H NMR experiments (ESI – section B.1†).

The ^{2}H NMR experiments were also used to determine the effect of KC2 and KC2H on the POPC bilayer structure. POPC/KC2 systems with four different mixing ratios (100/00, 90/10, 80/20, and 70/30) were studied at two pH levels (4.4 and 8.1), and at several temperatures ranging from 288 to 313 K (ESI – section C†).

Simulations using the validated models were used to study the POPC/KC2 binary mixtures as a function of pH and mixing ratio [Table S1] (ESI – section A.2†). Systems with all the aforementioned mixing ratios were simulated at acidic, neutral and basic pH levels. Considering the pK_a of ~6.7 for KC2, the simulated POPC/KC2 systems, where all the KC2 were taken as neutral, correspond to pH levels of 7.4 to 8.1. Also, the POPC/KC2H bilayers, with all the KC2 taken as protonated (KC2H), correspond to experimental systems at pH of ~4.

Based on the results from MD simulations, additional SAXS experiments, cryo-TEM experiments and simulations were designed and conducted. SAXS experiments were used to measure the bilayer repeat spacing (d-spacing) in the POPC/KC2 lamellar phase for several mixing ratios at basic pH values. Cryo-TEM experiments were conducted to detect possible KC2 segregation from POPC. In the cryo-TEM experiments, cholesterol was added to the POPC/KC2 and POPC/KC2H systems (ESI – section A.1.4†) as binary mixtures POPC/KC2 or POPC/KC2H yield particles too small to image. Details on both SAXS and cryo-TEM experiments are provided in the ESI.† To investigate the effect of cholesterol and bridge the cryo-TEM and SAXS/NMR experiments, POPC/KC2/cholesterol (25/30/45) systems corresponding to the mixing ratio used in the cryo-TEM experiments were simulated for pH levels of 4.0 and 7.4 [Table S1] (ESI – section A.2†).

Results and discussion

In simulations, starting from a binary lipid mixture composed of POPC and neutral KC2 in a bilayer form, almost all the neutral KC2 segregated from POPC and incorporated into the hydrophobic interior between the two POPC monolayers [Fig. 1a, pH 7.4]. In contrast, KC2H, with a net charge of +e, stays in the lipid–water interface and interacts with water molecules, ions, and POPC headgroups [Fig. 1a, pH 4], at all temperatures and mixing ratios studied [Table S1†]. These

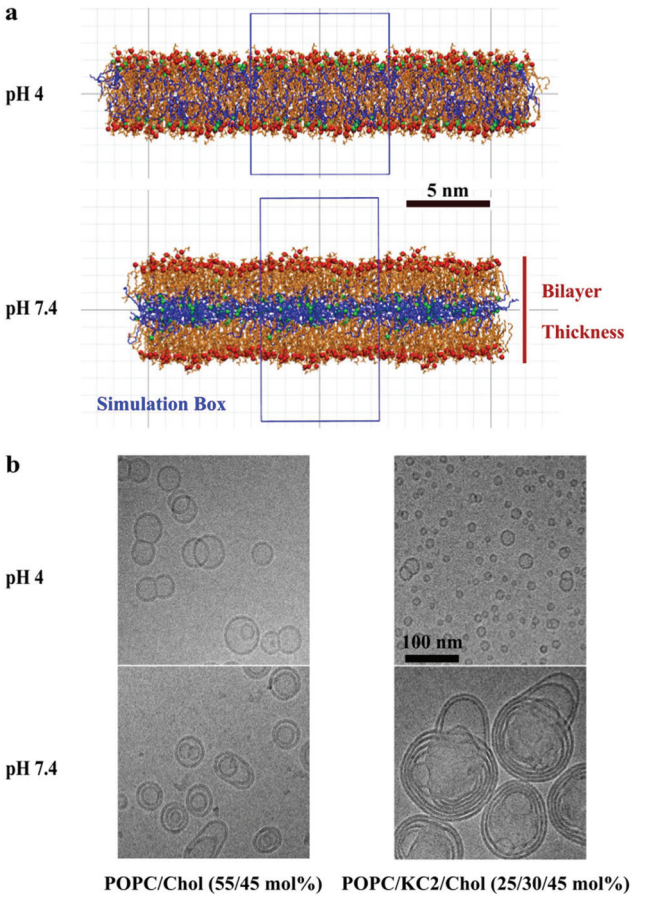

Fig. 1 KC2 segregation from POPC as a function of pH. (a) Bilayers are composed of POPC and KC2 or KC2H. Snapshots are taken from systems with 70 mol% POPC. Green and red spheres represent the nitrogen atoms of KC2 and phosphorus atoms of POPC, whereas the blue and orange lines are representative of KC2 and POPC acyl chains, respectively. For clarity, hydrogen atoms, ions, and water molecules are not shown. The simulation box is shown as a blue rectangle. The vertical line represents the phosphate–phosphate bilayer thickness defined as the ensemble averaged distance between the red spheres (phosphorus atoms of POPC) in the two leaflets. (b) Cryo-TEM micrographs of POPC/cholesterol (55/45) and POPC/KC2(H)/cholesterol (25/30/45) mixtures at pH 4.0 and 7.4.

observations in simulations were further investigated using cryo-TEM, ^{2}H NMR, and SAXS experiments.

The cryo-TEM micrographs of POPC/KC2/cholesterol dispersions are shown in Fig. 1b. These micrographs suggest that all particles regardless of KC2 content, displayed bilayer structures at pH 4.0, but not at pH 7.4. For systems with no KC2, raising the pH from 4.0 to 7.4 changed the particle structures from unilamellar vesicles to bi- and oligo-lamellar structures. When 30 mol% KC2 was added to the system, unilamellar vesicles but with qualitatively smaller sizes compared to the POPC/cholesterol dispersions were formed. However, at pH 7.4 larger multi-lamellar vesicles with electron-dense cores were formed. The appearance of this electron-dense core upon increasing pH level supports the idea that KC2 separates from POPC and cholesterol, and leading to the formation of the oily cores. Furthermore, systems with 30 mol% KC2 at pH 7.4 formed particles that were larger than those formed with the same composition at pH 4.0, implying that particle fusion has occurred.[14] Taken together, the separation of POPC and KC2 is supported by cryo-TEM images of POPC/KC2/cholesterol mixtures [Fig. 1b]. Note that systems studied by cryo-TEM containing cholesterol are different from POPC/KC2(H) dispersions studied in simulations. The addition of cholesterol to POPC/KC2(H) was necessary for the formation of nanoparticles that could be imaged easily (ESI – section A.1.1†). Moreover, these systems are more directly related to actual LNPs because cholesterol is a major component of LNPs.[3] We simulated POPC/KC2/cholesterol systems corresponding to the cryo-TEM experiments to determine whether the presence of cholesterol affects the KC2 segregation observed in the binary mixtures.

In the presence of 45% cholesterol in the simulations KC2 in its neutral form is confined in the bilayer interior, as observed in the binary mixtures [Fig. 2]. *Ca.* 2.2% of the cholesterols were incorporated into the hydrophobic interior and dissolved in the confined neutral KC2 lipids. Cholesterol solubility in KC2 oily core of LNPs has been previously suggested by Kulkarni *et al.*[14]

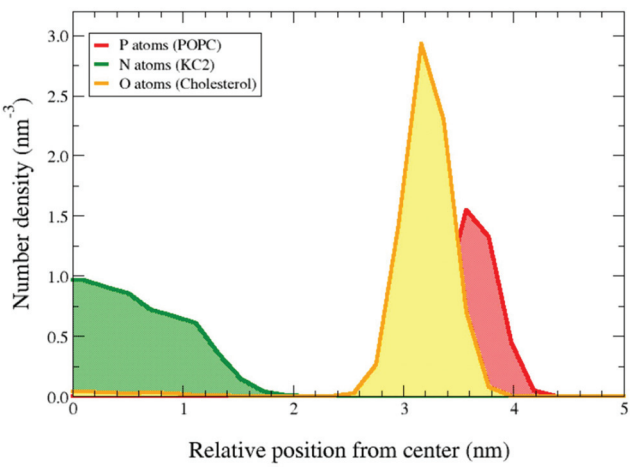

Fig. 2 KC2 confinement in presence of 45% cholesterol. The symmetrized number densities for the POPC phosphorus atoms, KC2 nitrogen atoms, and cholesterol oxygens in POPC/KC2/cholesterol (25/30/45) systems for pH = 7.4 at T = 313 K. The horizontal axis shows the distance from the mid-plane of the bilayer in the direction normal to the bilayer surface.

Order parameter (S_{CD}) profiles from ^{2}H NMR can also be used to characterize lipid organization and interactions in lipid mixtures. ^{2}H NMR S_{CD} profiles of POPC-d_{31}/KC2(H) systems are shown in Fig. S2 and S3.† At 288 K, adding KC2H to POPC-d_{31} increases palmitoyl chain order [Fig. S2†], implying that KC2H intercalates between POPC-d_{31} molecules as predicted by the MD simulations. In contrast, adding even 30 mol% KC2 to POPC-d_{31} has little to no effect on the conformational freedom of the palmitoyl chain. This suggests that KC2 does not interact with POPC-d_{31} chains to a significant extent, since KC2H does affect POPC-d_{31} palmitoyl chain order. Note, though, that it is possible for amphiphiles to intercalate among phospholipid chains without affecting chain order. For example, 25 mol% 1-decanol does not affect DPPC palmitoyl chain order parameters.[18,19] But given that KC2H significantly orders POPC-d_{31}, despite its charged dimethylamine, it is likely that KC2's lack of effect on POPC-d_{31} chain order stems from a lack of interaction with the chains. The observed differences between POPC/KC2(H) order parameter profiles at low and high pH become less significant with heating and are insignificant at 313 K [Fig. S3†], likely because thermal energy enhances chain fluctuations and loosens lateral packing.

Our SAXS results can also be interpreted to suggest that KC2 and POPC are segregated [Fig. S4†]. The broadening of scattering peaks upon the incorporation of KC2 implies that the lamellae are significantly less correlated than in pure POPC, as would be the case if they were interrupted by pools of KC2. As well, the increases in lamellar repeat spacing observed for POPC/KC2 multilamellar dispersions at pH 8.1 or 8.5 (ESI – section D†) are consistent with the interbilayer repulsion expected for the small amount of KC2H at these pH values.[20]

Both simulations and experiments suggest that KC2 separates from POPC, but the distribution of KC2 in the system is not the same between two approaches. In simulations, the segregated KC2 lipids are confined within the bilayer center. This confinement results in a systematic increase in the POPC inter-leaflet distance [Fig. 3]; from 3.72 nm to 4.18 nm, 4.44 nm, and 5.32 nm upon raising the KC2 molar fraction from 0% to 10%, 20%, and 30%, respectively. The KC2 incorporation in the bilayer center was not, however, supported by the SAXS experiments. Moreover, the neutral KC2 goes to the nano-formulation core in the cryo-TEM experiments [Fig. 1b]. This difference in KC2 distribution between simulations and experiments might be a direct effect of periodic boundary condition in the simulation. The complete separation of KC2 to the aqueous phase is not energetically favorable (or allowed) due to the applied boundary condition. Indeed, in the simulations confinement into the bilayer interior is the only possible scenario, unless a massive system is simulated that allows (energetically speaking) the KC2 expulsion from the bilayer.

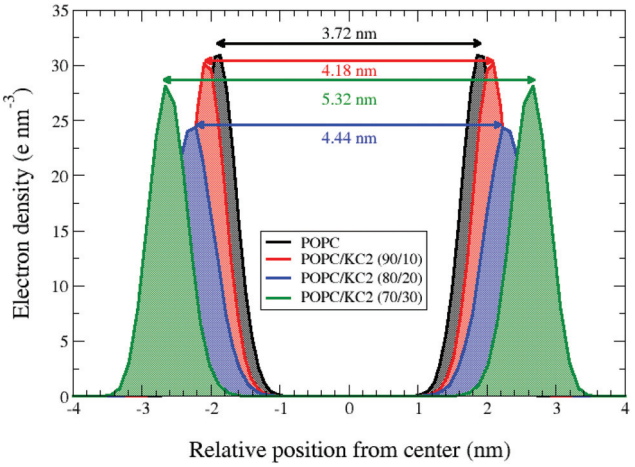

Fig. 3 Systematic increase in POPC inter-leaflet distance upon raising the KC2 concentration at basic pH. Symmetrized electron densities for the phosphorus atoms of POPC were calculated from the simulation for the systems with different mixing ratios at neutral/basic pH and T = 313 K. The horizontal axis shows the distance from the mid-plane of the bilayer in the direction normal to the bilayer surface. Each double-headed arrow represents the peak-to-peak distance for a mixing ratio, corresponding to the phosphate-to-phosphate (P–P) inter-leaflet distance. For the pure POPC at 313 K, the P–P distance is about 3.72 nm.

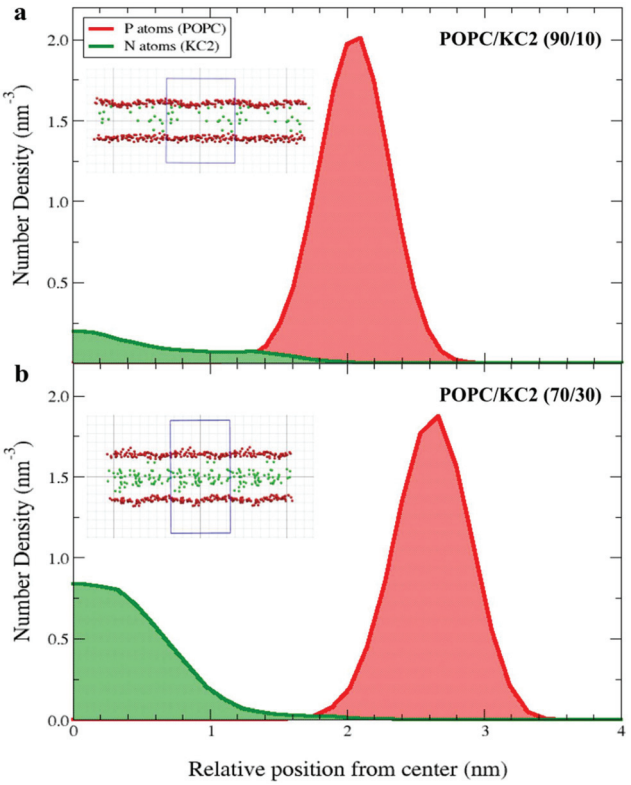

Fig. 4 KC2 confinement as a function of mixing ratio. The symmetrized number densities for the KC2 nitrogen atoms and POPC phosphorus atoms are shown at neutral/basic pH and T = 313 K for two mixing ratios: (a) POPC/KC2 (90/10), and (b) POPC/KC2 (70/30). The horizontal axis shows the distance from the mid-plane of the bilayer in the direction normal to the bilayer surface. The insets are snapshots taken from the corresponding systems. The red and green spheres represent the POPC phosphorus atoms and KC2 nitrogen atoms, respectively. The blue box represents the simulation box. Water, ions, and other atoms in POPC and KC2 are omitted for clarity. The system with 30 mol% KC2 seems to have proportionally less KC2 headgroups in the lipid–water interface (shown as the POPC phosphorus atom densities) compared to the system with 10 mol% KC2.

KC2 incorporation into the POPC bilayer center is not, however, impossible, and might be the case for systems with low KC2 concentrations. There are experimental reports on alkanes segregating into the middle of bilayers,[21] or into the voids in inverted hexagonal structures.[22] Furthermore, there are reports on the confinement of water-soluble polymers into the center of bilayers composed of non-ionic surfactants.[23] There are also computational studies where partitioning of hydrophobic alkanes and polymers in the bilayer interior has been reported.[24] Although there are numerous examples on partitioning of both small and large drug molecules into the lipid membranes,[25] there is no simple explanation for KC2 separation from PC lipids.

Simulations also suggest that the level of KC2 confinement was a function of KC2 concentration [Fig. 4]. That being said, the KC2 percentage confined in the hydrophobic section is higher for the system with a higher concentration of KC2. For the 10 mol% KC2, a few percent of the lipids could stay in the lipid–water interface but as the concentration of KC2 increased to 20 and 30 mol%, more and more KC2 were confined in the membrane center [Fig. 4].

These results suggest that an increase in pH from 4.4 to 7.4/8.1 causes the KC2 to separate from POPC. Results from POPC/KC2(H) and POPC/KC2(H)/cholesterol systems can be further related to the LNPs because phosphatidylcholine, KC2(H) and cholesterol are three major components of LNPs. Therefore, interactions between these molecules play critical roles on the internal structure and consequently the drug delivery efficacy of LNPs. However, LNPs are more complex and contain other molecules in their formulations. For instance, LNPs contain distearoylphosphatidylcholine (DSPC) which has two saturated acyl chains in contrast to POPC, and PEG-lipids which assist in stabilizing the LNPs.[3] These differences could result in different molecular behavior than what was observed in the simple model systems in this study.

Considering these limitations, our findings suggest that KC2 is the major component forming the oil droplets observed in the core of LNPs.[13,14] As proposed elsewhere,[14] these oil droplets are expected to be stabilized by a lipid monolayer on the surface. It is likely that the other components (DSPC/cholesterol/PEG-lipid) contribute to the formation of a stabilizing surface monolayer. It is hypothesized that the movement of deprotonated ionizable lipid from the surface layer to the core of the nanoparticle results in a drastic shift in the required surface to core lipid ratio to maintain a stable LNP. Thus, as the core lipid accumulates, particle fusion continues until the surface of the LNP is decorated with the required amount of

lipid to maintain structural integrity. As shown previously,[14] the amount of KC2 present in the formulation dictates the particle size.

The confinement of KC2 inside the LNP might also delay the detection of endosomal acidification, and a consequential delay in KC2 protonation and their transfer to the LNP surface. Lack of sufficient KC2H on the LNP's surface reduces the LNP's attachment to and effective interactions with negatively charged endosomal membrane.

Even though neutral KC2 segregates from POPC, KC2H stays in the POPC bilayer and interacts with other molecules in the lipid–water interface. Both ^{2}H NMR experiments and simulations suggest that including KC2H in the system slightly induces order in the POPC palmitoyl chain in a concentration-dependent way [Fig. S2 and S3†]. In simulations, KC2H left the P–P distance almost unaffected [Fig. S5†]. Moreover, adding KC2H to the systems attracted Cl^- ions to the membrane surface, and pushed the Na^+ ions far from the lipid–water interface [Fig. S6†]. It also affects the POPC choline group distribution which consequently affects the POPC P → N vector orientation [Fig. S7†]. These observations are consistent with the previous report on other zwitterionic–cationic lipid mixtures.[26]

Conclusions

Our results suggest neutral KC2 is segregated from POPC, while charged KC2H mixes with POPC in the lipid bilayer. KC2H affects the POPC head group orientation but had no effect on the bilayer thickness. The segregation of KC2 supports the recently proposed model for LNPs containing KC2.[14] The sequestration of KC2 from POPC might also explain why this class of LNPs suffers from low efficacy of drug release from endosomes.

Abbreviations

LNP	Lipid nanoparticle
ICL	Ionizable cationic lipid
^{2}H NMR	Deuterium nuclear magnetic resonance
MD	Molecular dynamics
S_{CD}	Deuterium order parameter for C–D bond
POPC	1-Palmitoyl-2-oleoyl-*sn-glycero*-3-phosphocholine
SAXS	Small angle X-ray scattering
KC2(H)	DLin-KC2-DMA ionizable cationic lipid
KC2H	The protonated form of KC2(H)
KC2	The neutral form of KC2(H)
Cryo-TEM	Cryogenic transmission electron microscopy
siRNA	Small interfering ribonucleic acid

Conflicts of interest

There are no conflicts of interest to declare.

Acknowledgements

This work was supported by a Natural Sciences and Engineering Council (Canada) Strategic Project Grant (DPT, JT) (STPGP/463247-2014). DPT is an Alberta Innovates Health Solutions Scientist and Alberta Innovates Technology Futures Strategic Chair in (Bio)Molecular Simulation. Further support came from the Canada Research Chairs Program (DPT). Simulations were carried out on Compute Canada facilities, supported by the Canada Foundation for Innovation and partners. PRC is funded by a Foundation grant (FDN 148469) from the Canadian Institutes of Health Research, and a British Columbia Innovation Council Ignite grant.

References

1 T. S. Zimmermann, A. C. Lee, A. Akinc, B. Bramlage, D. Bumcrot, M. N. Fedoruk, J. Harborth, J. A. Heyes, L. B. Jeffs, M. John and A. D. Judge, RNAi-mediated gene silencing in non-human primates, *Nature*, 2006, **441**(7089), 111–114.

2 M. Y. Arteta, T. Kjellman, S. Bartesaghi, S. Wallin, X. Wu, A. J. Kvist, A. Dabkowska, N. Székely, A. Radulescu, J. Bergenholtz and L. Lindfors, Successful reprogramming of cellular protein production through mRNA delivered by functionalized lipid nanoparticles, *Proc. Natl. Acad. Sci. U. S. A.*, 2018, **115**(15), E3351–E3360.

3 Y. Tam, S. Chen and P. R. Cullis, Advances in lipid nanoparticles for siRNA delivery, *Pharmaceutics*, 2013, **5**(3), 498–507.

4 C. Wan, T. M. Allen and P. R. Cullis, Lipid nanoparticle delivery systems for siRNA-based therapeutics, *Drug Delivery Transl. Res.*, 2014, **4**(1), 74–83.

5 J. Gilleron, W. Querbes, A. Zeigerer, A. Borodovsky, G. Marsico, U. Schubert, K. Manygoats, S. Seifert, C. Andree, M. Stöter and H. Epstein-Barash, Image-based analysis of lipid nanoparticle–mediated siRNA delivery, intracellular trafficking and endosomal escape, *Nat. Biotechnol.*, 2013, **31**(7), 638–646.

6 G. Sahay, W. Querbes, C. Alabi, A. Eltoukhy, S. Sarkar, C. Zurenko, E. Karagiannis, K. Love, D. Chen, R. Zoncu, Y. Buganim, *et al.*, Efficiency of siRNA delivery by lipid nanoparticles is limited by endocytic recycling, *Nat. Biotechnol.*, 2013, **31**(7), 653–658.

7 S. Chen, Y. Y. C. Tam, P. J. Lin, M. M. Sung, Y. K. Tam and P. R. Cullis, Influence of particle size on the in vivo potency of lipid nanoparticle formulations of siRNA, *J. Controlled Release*, 2016, **235**, 236–244.

8 I. Koltover, T. Salditt, J. O. Rädler and C. R. Safinya, An inverted hexagonal phase of cationic liposome-DNA complexes related to DNA release and delivery, *Science*, 1998, **281**(5373), 78–81.

9 H. Kim and C. Leal, Cuboplexes: Topologically active siRNA delivery, *ACS Nano*, 2015, **9**(10), 10214–10226.

10 S. C. Semple, A. Akinc, J. Chen, A. P. Sandhu, B. L. Mui, C. K. Cho, D. W. Sah, D. Stebbing, E. J. Crosley,

E. Yaworski, I. M. Hafez, *et al.*, Rational design of cationic lipids for siRNA delivery, *Nat. Biotechnol.*, 2010, **28**(2), 172–176.

11 M. Jayaraman, S. M. Ansell, B. L. Mui, Y. K. Tam, J. Chen, X. Du, D. Butler, L. Eltepu, S. Matsuda, J. K. Narayanannair and K. G. Rajeev, Maximizing the potency of siRNA lipid nanoparticles for hepatic gene silencing in vivo, *Angew. Chem., Int. Ed.*, 2012, **51**(34), 8529–8533.

12 C. L. Chan, R. N. Majzoub, R. S. Shirazi, K. K. Ewert, Y. J. Chen, K. S. Liang and C. R. Safinya, Endosomal escape and transfection efficiency of PEGylated cationic liposome–DNA complexes prepared with an acid-labile PEG-lipid, *Biomaterials*, 2012, **33**(19), 4928–4935.

13 A. K. Leung, I. M. Hafez, S. Baoukina, N. M. Belliveau, I. V. Zhigaltsev, E. Afshinmanesh, D. P. Tieleman, C. L. Hansen, M. J. Hope and P. R. Cullis, Lipid nanoparticles containing siRNA synthesized by microfluidic mixing exhibit an electron-dense nanostructured core, *J. Phys. Chem. C*, 2012, **116**(34), 18440–18450.

14 J. A. Kulkarni, M. M. Darjuan, J. E. Mercer, S. Chen, R. van der Meel, J. L. Thewalt, Y. Y. C. Tam and P. R. Cullis, On the formation and morphology of lipid nanoparticles containing ionizable cationic lipids and siRNA, *ACS Nano*, 2018, **12**(5), 4787–4795.

15 A. K. Leung, Y. Y. C. Tam, S. Chen, I. M. Hafez and P. R. Cullis, Microfluidic mixing: A general method for encapsulating macromolecules in lipid nanoparticle systems, *J. Phys. Chem. B*, 2015, **119**(28), 8698–8706.

16 N. M. Belliveau, J. Huft, P. J. Lin, S. Chen, A. K. Leung, T. J. Leaver, A. W. Wild, J. B. Lee, R. J. Taylor, Y. K. Tam and C. L. Hansen, Microfluidic synthesis of highly potent limit-size lipid nanoparticles for in vivo delivery of siRNA, *Mol. Ther.–Nucleic Acids*, 2012, **1**, e37.

17 J. B. Klauda, R. M. Venable, J. A. Freites, J. W. O'Connor, D. J. Tobias, C. Mondragon-Ramirez, I. Vorobyov, A. D. MacKerell Jr. and R. W. Pastor, Update of the CHARMM all-atom additive force field for lipids: Validation on six lipid types, *J. Phys. Chem. B*, 2010, **114**(23), 7830–7843.

18 J. L. Thewalt, S. R. Wassall, H. Gorrissen and R. J. Cushley, Deuterium NMR study of the effect of n-alkanol anesthetics on a model membrane system, *Biochim. Biophys. Acta, Biomembr.*, 1985, **817**(2), 355–365.

19 J. L. Thewalt, A. P. Tulloch and R. J. Cushley, A deuterium NMR study of labelled n-alkanol anesthetics in a model membrane, *Chem. Phys. Lipids*, 1986, **39**(1–2), 93–107.

20 B. P. Navas, K. Lohner, G. Deutsch, E. Sevcsik, K. A. Riske, R. Dimova, P. Garidel and G. Pabst, Composition dependence of vesicle morphology and mixing properties in a bacterial model membrane system, *Biochim. Biophys. Acta, Biomembr.*, 2005, **1716**(1), 40–48.

21 S. H. White, G. I. King and J. E. Cain, Location of hexane in lipid bilayers determined by neutron diffraction, *Nature*, 1981, **290**(5802), 161.

22 Z. Chen and R. P. Rand, Comparative study of the effects of several n-alkanes on phospholipid hexagonal phases, *Biophys. J.*, 1998, **74**(2), 944–952.

23 E. Z. Radlinska, T. Gulik-Krzywicki, F. Lafuma, D. Langevin, W. Urbach, C. E. Williams and R. Ober, Polymer confinement in surfactant bilayers of a lyotropic lamellar phase, *Phys. Rev. Lett.*, 1995, **74**(21), 4237–4240.

24 D. Bochicchio, E. Panizon, L. Monticelli and G. Rossi, Interaction of hydrophobic polymers with model lipid bilayers, *Sci. Rep.*, 2017, **7**(1), 6357.

25 R. M. Venable, A. Krämer and R. W. Pastor, Molecular dynamics simulations of membrane permeability, *Chem. Rev.*, 2019, **119**(9), 5954–5997.

26 A. A. Gurtovenko, M. Patra, M. Karttunen and I. Vattulainen, Cationic DMPC/DMTAP lipid bilayers: Molecular dynamics study, *Biophys. J.*, 2004, **86**(6), 3461–3472.